

# Effect of Shear viscosity on the nucleation of antikaon condensed matter in neutron stars

Sarmistha Banik<sup>1</sup> and Debades Bandyopadhyay<sup>2</sup>

<sup>1</sup>*Variable Energy Cyclotron Centre,*

*1/AF Bidhannagar, Kolkata-700064, India and*

<sup>2</sup>*Astroparticle Physics and Cosmology Division,*

*Saha Institute of Nuclear Physics, 1/AF Bidhannagar, Kolkata-700064, India*

## Abstract

We investigate a first-order phase transition from hadronic matter to antikaon condensed matter during the cooling stage of protoneutron stars. The phase transition proceeds through the thermal nucleation of antikaon condensed matter. In this connection we study the effect of shear viscosity on the thermal nucleation rate of droplets of antikaon condensed matter. Here we adopt the same equation of state for the calculation of shear viscosity and thermal nucleation time. We compute the shear viscosity of neutron star matter composed of neutrons, protons, electrons and muons using the relativistic mean field model. The prefactor in the nucleation rate which includes the shear viscosity, is enhanced by several orders of magnitude compared with the  $T^4$  approximation of earlier calculations. Consequently the thermal nucleation time in the  $T^4$  approximation overestimates our result. Further the thermal nucleation of an antikaon droplet might be possible in our case for surface tension smaller than  $20 \text{ MeV fm}^{-2}$ .

PACS numbers: 97.60.Jd, 26.60.-c, 52.25.Fi, 64.60.Q-

## I. INTRODUCTION

Antikaon ( $K^-$  meson) condensation in dense baryonic matter formed in heavy ion collisions as well as in neutron stars was first proposed by Kaplan and Nelson [1]. There was lots of interest in the study of antikaon condensation in neutron stars [2–16] after their work. A first-order phase transition from hadronic matter to antikaon condensed matter was investigated in several cases using relativistic field theoretical models [7, 11, 15, 16]. The phase transition was either studied using Maxwell construction or governed by Gibbs’ rules for phase equilibrium along with global baryon number and charge conservation [17]. In those cases the focus was on the equation of state (EoS) and neutron star structure as well as critical temperature of antikaon condensation.

A first-order phase transition may proceed through the nucleation of droplets of the new phase. The formation of droplets of exotic matter such as antikaon condensed matter and quark matter, could be possible in neutron stars when the protoneutron star cools down to a temperature of  $\sim 10$  MeV and is deleptonised [18–23]. This nucleation process could be due to quantum and thermal nucleation mechanisms [22]. The thermal nucleation of antikaon condensed matter was already studied using the homogeneous nucleation theory of Langer [18, 19, 24]. Recently it has been shown in the context of nucleation of quark matter in hot and neutrino-free neutron stars that the thermal nucleation is more efficient than the quantum nucleation process at higher temperatures [22].

The homogeneous nucleation theory of Langer [24, 25] is applicable close to a first-order phase transition. The hadronic matter becomes metastable near the phase transition point when there is a sudden change in state variables. In this case thermal and quantum fluctuations play important roles in the metastable phase. Small ranged and localised fluctuations in state variables of the metastable hadronic matter might lead to the nucleation of droplets of stable antikaon condensed matter. Those droplets of the stable phase having radii larger than a critical radius will survive and grow. A droplet may grow beyond the critical size if the latent heat is transported from the surface of the droplet into the metastable phase. It was argued that the heat transportation could be achieved through the thermal dissipation and viscous damping [25–27]. The influence of thermal conductivity and shear viscosity on the thermal nucleation time was studied in a first-order phase transition from hadronic to quark matter [22, 26]. However there is no such calculation for the thermal nucleation of

antikaon condensed matter.

We are motivated to study the effect of shear viscosity on the thermal nucleation rate of droplets of antikaon condensed matter in this work. Shear viscosity of pure neutron and neutron star matter has been calculated by several groups [28–33]. Recently we have investigated the shear viscosity in antikaon condensed matter [34]. Though we considered a first-order antikaon condensation, we did not take into account the nucleation process. We performed the calculation of shear viscosity in neutron star matter using the EoS derived from relativistic field theoretical models. Now the question is how this shear viscosity of nucleonic phase may impact the nucleation of antikaon condensed phase. The earlier calculation of the nucleation of quark matter adopted a parametrised form of the shear viscosity [22]. In this calculation we adopt the same EoS for the computation of thermal nucleation time of the antikaon condensed phase and shear viscosity of nuclear matter.

We organise the paper in the following way. We describe models for homogeneous nucleation, shear viscosity and EoS in Sec. II. Results of this calculation are discussed in Sec. III. Sec. IV gives the summary and conclusions.

## II. FORMALISM

We consider a first-order phase transition from the charge neutral and beta-equilibrated nuclear matter to  $K^-$  condensed matter in a hot neutron star after the emission of trapped neutrinos. Droplets of antikaon condensed phase are formed in the metastable nuclear matter due to thermal fluctuations. Droplets of antikaon condensed matter above a critical size are of interest because those critical droplets will drive the phase transition. We adopt the homogeneous nucleation formalism of Langer to calculate the thermal nucleation rate [24]. In this formalism, the thermal nucleation per unit time per unit volume is given by [24, 25]

$$\Gamma = \Gamma_0 \exp \left( -\frac{\Delta F(R_c)}{T} \right) , \quad (1)$$

where  $\Delta F$  is the change in the free energy to produce a critical droplet in the metastable nuclear matter. The change in free energy of the system due to the formation of a droplet is given by [21, 23]

$$\Delta F(R) = -\frac{4\pi}{3}(P^K - P^N)R^3 + 4\pi\sigma R^2 , \quad (2)$$

where  $R$  is the radius of the droplet,  $\sigma$  is surface tension of the interface separating two phases and  $P^N$  and  $P^K$  are the pressure in nuclear and antikaon condensed phases respectively. We obtain the critical radius of the droplet from the maximum of  $\Delta F(R)$  i.e.  $\delta_R \Delta F = 0$  and it is

$$R_C = \frac{2\sigma}{(P^K - P^N)} . \quad (3)$$

The EoS enters into this calculation through the difference in pressures of two phases.

The prefactor in Eq. (1) is factorised in the following way [25–27]

$$\Gamma_0 = \frac{\kappa}{2\pi} \Omega_0 . \quad (4)$$

The statistical prefactor ( $\Omega_0$ ) gives the available phase space around the saddle point at  $R_C$  during the passage of the droplet through it. The expression for the statistical prefactor is

$$\Omega_0 = \frac{2}{3\sqrt{3}} \left( \frac{\sigma}{T} \right)^{3/2} \left( \frac{R_C}{\xi} \right)^4 , \quad (5)$$

Here  $\xi$  is the correlation length for kaons. This correlation length is considered to be the width of the interface between nuclear and antikaon condensed matter. Next we focus on the dynamical prefactor  $\kappa$ . This prefactor is responsible for the initial exponential growth rate of a critical droplet. It is given by [26, 27]

$$\kappa = \frac{2\sigma}{R_C^3 (\Delta w)^2} \left[ \lambda T + 2 \left( \frac{4}{3} \eta + \zeta \right) \right] . \quad (6)$$

Here  $\Delta w = w_K - w_N$  is the enthalpy difference of two phases whereas  $\lambda$  is thermal conductivity and  $\eta$  and  $\zeta$  are the shear and bulk viscosities of nuclear matter. It was shown that the latent heat would be taken away from the surface of the droplet due thermal dissipation and viscous damping [26, 27].

Finally the thermal nucleation time ( $\tau_{th}$ ) in the interior of neutron stars is calculated as

$$\tau_{th} = (V\Gamma)^{-1} , \quad (7)$$

where the volume  $V = 4\pi/3 R_{nuc}^3$ . We assume that pressure and temperature are constant within this volume in the core. It is evident from Eq. (7) that the thermal nucleation time is inversely proportional to transport coefficients. In connection with the quark matter nucleation, it was noted that the contribution of thermal conductivity is not appreciable. Further, we know that shear viscosity increases [34] and bulk viscosity decreases [35] as

temperature decreases. After the emission of neutrinos a hot neutron star cools down, and the thermal nucleation drives the phase transition when the temperature is  $\sim 10$  MeV. In this temperature regime, shear viscosity might be an important factor.

Now we focus on the calculation of shear viscosity in neutron star matter. It was noted that the main contributions to the total shear viscosity in neutron star matter came from electrons, the lightest charged particles, and neutrons, the most abundant particles [28–30, 32, 33]. Recently the proton shear viscosity, though small, was considered in our calculation [34]. We calculate shear viscosities for different particle species using coupled Boltzmann transport equations [29, 32, 34]. The effects of the exchange of transverse plasmons in the collisions of charged particles are included in this case [32, 36]. The knowledge of nucleon-nucleon scattering cross sections derived in the Dirac-Brueckner approach [37, 38] is used for the calculation of neutron and proton shear viscosities [32, 34, 39]. Contributions of neutrons, protons, electrons and muons to the total shear viscosity

$$\eta_{total} = \eta_n + \eta_p + \eta_e + \eta_\mu , \quad (8)$$

are given by [32, 34]

$$\eta_{i(=n,p,e,\mu)} = \frac{n_i p_{F_i}^2 \tau_i}{5m_i^*} . \quad (9)$$

Here  $\tau_i$  is the relaxation time of  $i$ -th species as calculated in Ref. [32, 34]. Effective mass and Fermi momentum of  $i$ -th particle species are denoted by  $m_i^*$  and  $p_{F_i}$ , respectively. For electrons and muons, effective masses are taken as their chemical potentials due to relativistic effects. We adopt a relativistic field theoretical model which is described in the following paragraphs, for the calculation effective masses and Fermi momenta of neutrons and protons.

Besides the computation of shear viscosities, the knowledge of the EoS is essential for the thermal nucleation rate. We note that the EoS enters into the calculation of thermal nucleation rate as given by Eqs. (1)-(3). We adopt relativistic field theoretical models to describe the  $\beta$  equilibrated matter in nuclear and antikaon condensed phases. Those two phases are composed of neutrons, protons, electrons, muons and of  $K^-$  mesons only in the antikaon condensed phase. Both phases are governed by baryon number conservation and charge neutrality conditions [17]. The baryon-baryon interaction mediated by the exchange

of  $\sigma$ ,  $\omega$  and  $\rho$  mesons is described by the Lagrangian density [9, 40–42]

$$\begin{aligned}\mathcal{L}_N = & \sum_{B=n,p} \bar{\psi}_B (i\gamma_\mu \partial^\mu - m_B + g_{\sigma B}\sigma - g_{\omega B}\gamma_\mu \omega^\mu - g_{\rho B}\gamma_\mu \mathbf{t}_B \cdot \boldsymbol{\rho}^\mu) \psi_B \\ & + \frac{1}{2} (\partial_\mu \sigma \partial^\mu \sigma - m_\sigma^2 \sigma^2) - U(\sigma) \\ & - \frac{1}{4} \omega_{\mu\nu} \omega^{\mu\nu} + \frac{1}{2} m_\omega^2 \omega_\mu \omega^\mu - \frac{1}{4} \boldsymbol{\rho}_{\mu\nu} \cdot \boldsymbol{\rho}^{\mu\nu} + \frac{1}{2} m_\rho^2 \boldsymbol{\rho}_\mu \cdot \boldsymbol{\rho}^\mu .\end{aligned}\quad (10)$$

The scalar self-interaction term [9, 42, 43] is

$$U(\sigma) = \frac{1}{3} g_1 m_N (g_{\sigma N} \sigma)^3 + \frac{1}{4} g_2 (g_{\sigma N} \sigma)^4 , \quad (11)$$

The effective nucleon mass is given by  $m_B^* = m_B - g_{\sigma B}\sigma$ , where  $m_B$  is the vacuum baryon mass. The Lagrangian density for (anti)kaons in the minimal coupling is given by [7, 10, 12]

$$\mathcal{L}_K = D_\mu^* \bar{K} D^\mu K - m_K^{*2} \bar{K} K , \quad (12)$$

where the covariant derivative is  $D_\mu = \partial_\mu + ig_{\omega K}\omega_\mu + ig_{\rho K}\mathbf{t}_K \cdot \boldsymbol{\rho}_\mu$  and the effective mass of (anti)kaons is  $m_K^* = m_K - g_{\sigma K}\sigma$ . The in-medium energy of  $K^-$  mesons is given by

$$\omega_{K^-} = \sqrt{(p^2 + m_K^{*2})} - \left( g_{\omega K}\omega_0 + \frac{1}{2} g_{\rho K}\rho_{03} \right) . \quad (13)$$

We consider the s-wave ( $\mathbf{p} = 0$ ) condensation. The condensation sets in when the chemical potential of  $K^-$  mesons ( $\mu_{K^-} = \omega_{K^-}$ ) is equal to the electron chemical potential i.e.  $\mu_e = \mu_{K^-}$ . The critical droplet of antikaon condensed matter is in total phase equilibrium with the metastable nuclear matter. The mixed phase is governed by Gibbs' phase rule along with global baryon number conservation and charge neutrality [17]. Two phases are in chemical equilibrium and the mechanical equilibrium is constrained by Eq. (3).

We do not consider the variation of the meson fields in the droplet with position. This is known as the bulk approximation [19]. We solve equations of motion self-consistently in the mean field approximation [40] and find effective masses and Fermi momenta of baryons. Further we obtain the pressure in nuclear matter ( $P^N$ ) and in antikaon condensed matter ( $P^K$ ) as given by Ref.[12].

### III. RESULTS AND DISCUSSIONS

We adopt the Glendenning and Moszkowski parameter set known as GM1 [44] for nucleon-meson coupling constants which are obtained by reproducing the saturation properties of

nuclear matter such as binding energy  $E/B = -16.3$  MeV, baryon density  $n_0 = 0.153$  fm $^{-3}$ , asymmetry energy coefficient  $a_{\text{asy}} = 32.5$  MeV, incompressibility  $K = 300$  MeV and effective nucleon mass  $m_N^*/m_N = 0.70$ . Next we determine kaon-meson vector coupling constants using the quark model and isospin counting rule [7, 34]. And the scalar kaon-meson coupling constant is obtained from the real part of  $K^-$  optical potential depth at normal nuclear matter density.

Heavy ion collision experiments and  $K^-$  atomic data indicated an attractive potential for antikaons and a repulsive potential for kaons [45–50]. However the strength of antikaon optical potential depth is a debatable issue. It was found from the analysis of  $K^-$  atomic data that the real part of the antikaon optical potential could be as large as  $U_{\bar{K}} = -180 \pm 20$  MeV at normal nuclear matter density [45, 46]. But theoretical models including chirally motivated coupled channel models as well as double pole structure of  $\Lambda(1405)$  could not find such a strongly attractive antikaon optical potential depth [51–54]. In this calculation we take an antikaon optical potential depth of  $U_{\bar{K}} = -160$  MeV at normal nuclear matter density and obtain the kaon-scalar meson coupling constant  $g_{\sigma K} = 2.9937$ .

Here we study the thermal nucleation of antikaon condensed phase after the emission of trapped neutrinos followed by the evolution of a hot neutron star to the cold star. The stellar matter is heated during the diffusion of trapped neutrinos leading to the deleptonisation and maximum entropy per baryon  $s = 2$ . It would take about a few  $10^2$  s for the maximally heated star to cool down to a temperature  $\sim 1$  MeV. The threshold for the appearance of antikaon condensate would be reduced after the deleptonisation. We demonstrate this evolution of a neutrino-free neutron star with a few snap-shots corresponding to entropy per baryon  $s = 0, 1$ , and  $2$ . We adopt the finite temperature calculation of Ref.[16] in this case. We show the temperature as a function of baryon density in nuclear matter for fixed  $s = 1$  and  $2$  in Fig. 1. The temperature increases with baryon density. This shows that the temperature varies from a higher value in the core to a smaller value at the surface of a neutron star. The equations of state of neutrino free nuclear matter at fixed  $s = 0, 1$ , and  $2$  are exhibited in Fig. 2. It is evident from Fig. 2 that the temperature of a few tens of MeV does not modify the EoS appreciably upto energy densities  $\sim 1000$  MeV fm $^{-3}$  relevant at the center of a neutron star, with respect to the zero temperature EoS corresponding to the  $s = 0$ , case because the temperature is much less than the baryon chemical potential. Therefore, we consider the zero temperature EoS for the rest of our calculation.

The total shear viscosity in nuclear matter is shown as a function of normalised baryon density for different temperatures in Fig. 3. The shear viscosity decreases as temperature increases. Further, the shear viscosity increases with increasing baryon density. It was earlier noted that the temperature dependence of shear viscosities corresponding to different particle species was a complicated one and manifested through relaxation times [34]. This temperature dependence deviates from the characteristic temperature dependence,  $1/T^2$ , of a Fermi liquid [32]. Figure 3 shows the total shear viscosity for three temperatures  $T = 1, 10, \text{ and } 30 \text{ MeV}$ . We are interested in the temperature range from a few MeV to a few tens of MeV in this calculation.

Next our focus is on the prefactor ( $\Gamma_0$ ) of Eq. (4) which not only involves transport properties of nuclear matter such as thermal conductivity and shear and bulk viscosities but also depends on the correlation length of kaons and surface tension. The radius of the droplet is to be greater than the correlation length for kaons  $\xi$ . Otherwise many approximations in this calculation would collapse [19, 26]. The correlation length is also taken as the thickness of the interface between nuclear and kaon phases [22, 26] estimated to be  $\sim 5 \text{ fm}$  [19]. Here we consider antikaon droplets with radii greater than  $5 \text{ fm}$ . The other important parameter in the prefactor is the surface tension. The surface tension between nuclear and kaon phases was already calculated by Christiansen and collaborators [55]. They found that the surface tension varied from a value of  $30 \text{ MeV fm}^{-2}$  at the start of the mixed phase to a value of  $10 \text{ MeV fm}^{-2}$  at the end of the mixed phase. It is evident from the fit of Ref.[55] that the surface tension is sensitive to the EoS. It is to be noted that we have a different parameter set and stiffer EoS than those of Ref.[55]. We perform this calculation for a set of values of surface tension  $\sigma = 10, 15 \text{ and } 20 \text{ MeV fm}^{-2}$ . Further, we approximate the difference in enthalpy densities ( $\Delta w$ ) in Eq. (6) as the difference of energy densities because the pressure difference is negligible compared with the difference in energy densities [26].

The prefactor ( $\Gamma_0$ ) is shown as a function of temperature in Fig. 4. The prefactor is calculated at a baryon density  $n_b = 2.3n_0$  and surface tension  $\sigma = 10 \text{ MeV fm}^{-2}$ . The density chosen here is just above the critical density for the transition. We calculate the prefactor for two values of correlation length  $\xi = 2 \text{ and } 5 \text{ fm}$ . Solid lines correspond to the calculation of prefactor including the shear viscosity term and neglecting the thermal conductivity and bulk viscosity terms in Eq. (6). On the other hand, dashed lines imply the prefactor including only the thermal conductivity term. The thermal conductivity is



calculated according to Ref.[39]. The prefactor involving the shear viscosity term is a few orders of magnitude higher than that of the thermal conductivity for both values of kaon correlation length. It is worth mentioning here that the contributions of thermal conductivity and bulk viscosity in the prefactor were neglected in an earlier calculation of quark matter nucleation [22]. We observe that the prefactor for  $\xi = 5$  fm is substantially reduced from that of  $\xi = 2$  fm in both cases. In the following paragraphs we discuss the results of our calculation performed with the prefactor involving only the shear viscosity term.

The prefactor of Eq. (4) was approximated by  $T^4$  according to the dimensional analysis in some calculations [23, 26]. This approximation might differ considerably from the actual calculation of the prefactor. Fig. 5 shows the prefactor of Eq. (4) including only the contribution of shear viscosity along with the prefactor approximated by  $T^4$  as a function of temperature. It is evident from Figure 5 that the approximated prefactor is several orders of magnitude smaller than the prefactor calculated according to Eq. (4) at lower temperatures. However, this difference between two calculations is reduced appreciably at higher temperatures. It remains to be seen how two calculations of the prefactor influence the thermal nucleation time.

Now we discuss the nucleation time of a critical droplet of antikaon condensed matter calculated with the prefactor of Eq. (4) involving only the shear viscosity contribution. The critical radius of the droplet is obtained from the relation in Eq. (3). The droplet which overcomes the maximum height of the energy barrier of Eq. (1) occurring at the critical radius, grows exponentially. Such a droplet triggers the onset of antikaon condensation in the interior of a neutron star. For surface tension  $\sigma = 10$  MeV fm<sup>-2</sup>, we obtain an antikaon droplet with critical radius 6.32 fm at baryon density  $2.3n_0$ . This density is just above the critical density for transition from nuclear matter to the droplet of antikaon condensed matter where the volume fraction of the antikaon condensed phase is approaching zero. We perform the calculation of thermal nucleation of the critical droplet within a volume with  $R_{nuc} = 100$  m in the core of a neutron star as mentioned in Eq. (7). It is assumed that density, pressure and temperature are constant within this volume. The thermal nucleation time is plotted with temperature in Fig. 6. Results shown here are calculated with the kaon correlation length  $\xi = 5$  fm. For the above-mentioned case, the nucleation time of the critical droplet drops as temperature increases. For the case of  $\sigma = 10$  MeV fm<sup>-2</sup>, the nucleation time is 1 s at a temperature of  $T \sim 10$  MeV. We also estimate thermal

nucleation times of critical antikaon droplets for two other values of surface tension  $\sigma = 15$  and  $20 \text{ MeV fm}^{-2}$ . It is noted that the size of the critical droplet increases with increasing surface tension. Radii of the critical droplets are 9.48 and 12.6 fm corresponding to  $\sigma = 15$  and  $20 \text{ MeV fm}^{-2}$ , respectively, at a density  $2.3n_0$ . We find a similar trend of the nucleation time with temperature in these cases. However, the temperature corresponding to a particular nucleation time for example, 1 s, increases as the surface tension increases. It is worth mentioning here that the condensate might melt if the temperature is higher than the critical temperature [16]. We compare thermal nucleation times corresponding to different values of the surface tension with the cooling time of a protoneutron star  $t_{cool} \sim$  a few  $10^2$  s. Thermal nucleation of the antikaon condensed phase may be possible when the thermal nucleation time is less than the cooling time. It is evident from Fig. 6 that the thermal nucleation time is strongly dependent on the surface tension. Thermal nucleation of an antikaon droplet is a possibility for surface tension  $\sigma < 20 \text{ MeV fm}^{-2}$  because in this case the thermal nucleation time is less than the cooling time at a temperature which might be below the critical temperature of antikaon condensation [16]. We repeat the calculation of the thermal nucleation time with the correlation length  $\xi = 2 \text{ fm}$  and find that the thermal nucleation time is slightly higher than that of  $\xi = 5 \text{ fm}$  over the whole temperature regime considered here.

We compare the results of thermal nucleation time taking into account the effect of shear viscosity in the prefactor with that of the prefactor approximated by  $T^4$ . These results are shown in Fig. 7 for surface tension  $\sigma = 10 \text{ MeV fm}^{-2}$  and at a density  $n_b = 2.30n_0$ . The results of the  $T^4$  approximation are a few orders of magnitude higher than those of our calculation. For example, the thermal nucleation time is 1 s at  $T \sim 10 \text{ MeV}$  in our case, whereas it is  $\sim 10^3$  s at the same temperature for the  $T^4$  approximated case. These results demonstrate the importance of including the shear viscosity in the prefactor of Eq. (4) in the calculation of thermal nucleation time.

#### IV. SUMMARY AND CONCLUSIONS

We have investigated the first-order phase transition from nuclear matter to antikaon condensed matter through the thermal nucleation of a critical droplet of antikaon condensed matter. Our main focus in this calculation is the role of shear viscosity in the prefactor and

its consequences on the thermal nucleation rate. We adopt the same EoS derived in the relativistic mean field model for the calculation of shear viscosity and thermal nucleation rate. In this connection, we have constructed critical droplets of antikaon condensed matter above the critical density for different values of surface tension. Droplet radii increase with increasing surface tension. We obtain thermal nucleation time as a function of temperature for a set of values of surface tension and find that the thermal nucleation time is strongly dependent on the surface tension. Our results show that thermal nucleation of a critical antikaon droplet could be possible during the cooling stage of a hot neutron star after neutrinos are emitted for a lower value of surface tension  $\sigma < 20 \text{ MeV fm}^{-2}$ . Further, a comparison of our results with that of the  $T^4$  approximation shows that the  $T^4$  approximation overestimates our results of thermal nucleation time. This comparison highlights the importance of shear viscosity in our calculation.

We have considered the thermal nucleation in a nonrotating neutron star and neglected the bulk viscosity in the prefactor. However neutron stars rotate very fast at birth. They emit gravitational waves and become r-mode unstable [35]. The bulk viscosity plays an important role in damping the r-mode instability. The bulk viscosity might dominate over the shear viscosity above 10 MeV [35]. It would be interesting to investigate the effect of bulk viscosity on the thermal nucleation time in a rotating neutron star along with that of shear viscosity.

## V. ACKNOWLEDGEMENT

S.B. thanks the Alexander von Humboldt Foundation for the support during her visit at the Frankfurt Institute for Advanced Studies (FIAS).

- 
- [1] D.B. Kaplan and A.E. Nelson, Phys. Lett. B **175**, 57 (1986);  
A.E. Nelson and D.B. Kaplan, Phys. Lett. B **192**, 193 (1987).
  - [2] G.E. Brown, K. Kubodera, M. Rho and V. Thorsson, Phys. Lett. B **291**, 355 (1992).
  - [3] V. Thorsson, M. Prakash and J.M. Lattimer, Nucl. Phys. **A572**, 693 (1994).
  - [4] P.J. Ellis, R. Knorren and M. Prakash, Phys. Lett. B **349**, 11 (1995).
  - [5] C.-H. Lee, G.E. Brown, D.-P. Min and M. Rho, Nucl. Phys. A585 (1995) 401.

- [6] M. Prakash, I. Bombaci, M. Prakash, P.J. Ellis, J.M. Lattimer and R. Knorren, Phys. Rep. **280**, 1 (1997).
- [7] N.K. Glendenning and J. Schaffner-Bielich, Phys. Rev. C **60**, 025803 (1999).
- [8] R. Knorren, M. Prakash and P.J. Ellis, Phys. Rev. C **52**, 3470 (1995).
- [9] J. Schaffner and I.N. Mishustin, Phys. Rev. C **53**, 1416 (1996).
- [10] S. Pal, D. Bandyopadhyay and W. Greiner, Nucl. Phys. **A674**, 553 (2000).
- [11] S. Banik and D. Bandyopadhyay, Phys. Rev. C **63**, 035802 (2001).
- [12] S. Banik and D. Bandyopadhyay, Phys. Rev. C **64**, 055805 (2001).
- [13] S. Banik and D. Bandyopadhyay, Phys. Rev. C **66**, 065801 (2002).
- [14] S. Banik and D. Bandyopadhyay, Phys. Rev. D **67**, 123003 (2003).
- [15] J.A. Pons, S. Reddy, P.J. Ellis, M.Prakash, and J.M. Lattimer, Phys. Rev. C **62** 035803 (2000).
- [16] S. Banik, W. Greiner and D. Bandyopadhyay, Phys. Rev. C **78**, 065804 (2008).
- [17] N.K. Glendenning, Phys. Rev. D **46**, 1274 (1992).
- [18] T. Norsen, Phys. Rev. C **65**, 045805 (2002).
- [19] T. Norsen and S. Reddy, Phys. Rev. C **63**, 065804 (2001).
- [20] K. Iida and K. Sato, Phys. Rev. C **58**, 2538 (1998).
- [21] H. Heiselberg, in International Symposium on Strangeness and Quark Matter, edited by G. Vassiliadis, A. D. Panagiotou, S. Kumar and J. Madsen (World Scientific, Singapore, 1995) p. 338.
- [22] I. Bombaci, D. Logoteta, P.K. Panda, C. Providencia and I. Vidana, Phys. Lett. B **680** 448 (2009).
- [23] B.W. Mintz, E. Fraga, G. Pagliara and J. Schaffner-Bielich, Phys. Rev. D **81**, 123012 (2010).
- [24] J.S. Langer, Ann. Phys. (Paris) **54**, 258 (1969).
- [25] L.A. Turski and J.S. Langer, Phys. Rev. A **22**, 2189 (1980).
- [26] L.P. Csernai and J.I Kapusta, Phys. Rev. D **46**, 1379 (1992).
- [27] R. Venugopalan and A.P. Vischer, Phys. Rev. E **49**, 5849 (1994).
- [28] E. Flowers and N. Itoh, Astrophys. J. **206**, 218 (1976).
- [29] E. Flowers and N. Itoh, Astrophys. J. **230**, 847 (1979).
- [30] C. Cutler and L. Lindblom, Astrophys. J. **314**, 234 (1987).
- [31] O. Benhar and M. Valli, Phys. Rev. Lett. **99**, 232501 (2007).
- [32] P. S. Shternin and D. G. Yakovlev, Phys. Rev. **D78**, 063006 (2008).

- [33] N. Andersson, G. L. Comer and K. Glampedakis, Nucl. Phys. **A763**, 212 (2005).
- [34] R. Nandi, S. Banik and D. Bandyopadhyay, Phys. Rev. D **80**, 123015 (2009).
- [35] D. Chatterjee and D. Bandyopadhyay, Phys. Rev. D **74** 023003, (2006).
- [36] P. S. Shternin and D. G. Yakovlev, Phys. Rev. **D75**, 103004 (2007).
- [37] G.Q. Li and R. Machleidt, Phys. Rev. **C48**, 1702 (1993).
- [38] G.Q. Li and R. Machleidt, Phys. Rev. **C49**, 566 (1994).
- [39] D. A. Baiko, P. Haensel and D. G. Yakovlev, Astron. Astrophys. **374**, 151 (2001).
- [40] J. D. Walecka, Ann. of Phys. (N.Y.) **83**, 491 (1974).
- [41] B. D. Serot, Phys. Lett. **86B**, 146 (1979).
- [42] N. K. Glendenning, Phys. Lett. **114B**, 392 (1982).
- [43] J. Boguta and A. R. Bodmer, Nucl. Phys. **A292**, 413 (1977).
- [44] N.K. Glendenning and S.A. Moszkowski, Phys. Rev. Lett. **67**, 2414 (1991).
- [45] E. Friedman, A. Gal and C.J. Batty, Nucl. Phys. **A579**, 518 (1994);  
C.J. Batty, E. Friedman and A. Gal, Phys. Rep. **287**, 385 (1997).
- [46] E. Friedman, A. Gal, J. Mareš and A. Cieplý, Phys. Rev. **C60**, 024314 (1999).
- [47] V. Koch, Phys. Lett. **B337**, 7 (1994).
- [48] T. Waas and W. Weise, Nucl. Phys. **A625**, 287 (1997).
- [49] G.Q. Li, C.-H. Lee and G.E. Brown, Phys. Rev. Lett. **79**, 5214 (1997); Nucl. Phys. **A625**,  
372 (1997).
- [50] S. Pal, C.M. Ko, Z. Lin and B. Zhang, Phys. Rev. **C62**, 061903(R) (2000).
- [51] A. Ramos and E. Oset, Nucl. Phys. **A671**, 481 (2000).
- [52] J. Schaffner-Bielich, V. Koch and M. Effenberger, Nucl. Phys. **A669**, 153 (2000).
- [53] V.K. Magas, E. Oset and A. Ramos, Phys. Rev. Lett. **95**, 052301 (2005).
- [54] T. Hyodo and W. Weise, Phys. Rev. **C77**, 035204 (2008).
- [55] M.B. Christiansen, N.K. Glendenning and J. Schaffner-Bielich, Phys. Rev. C **62**, 025804  
(2000).

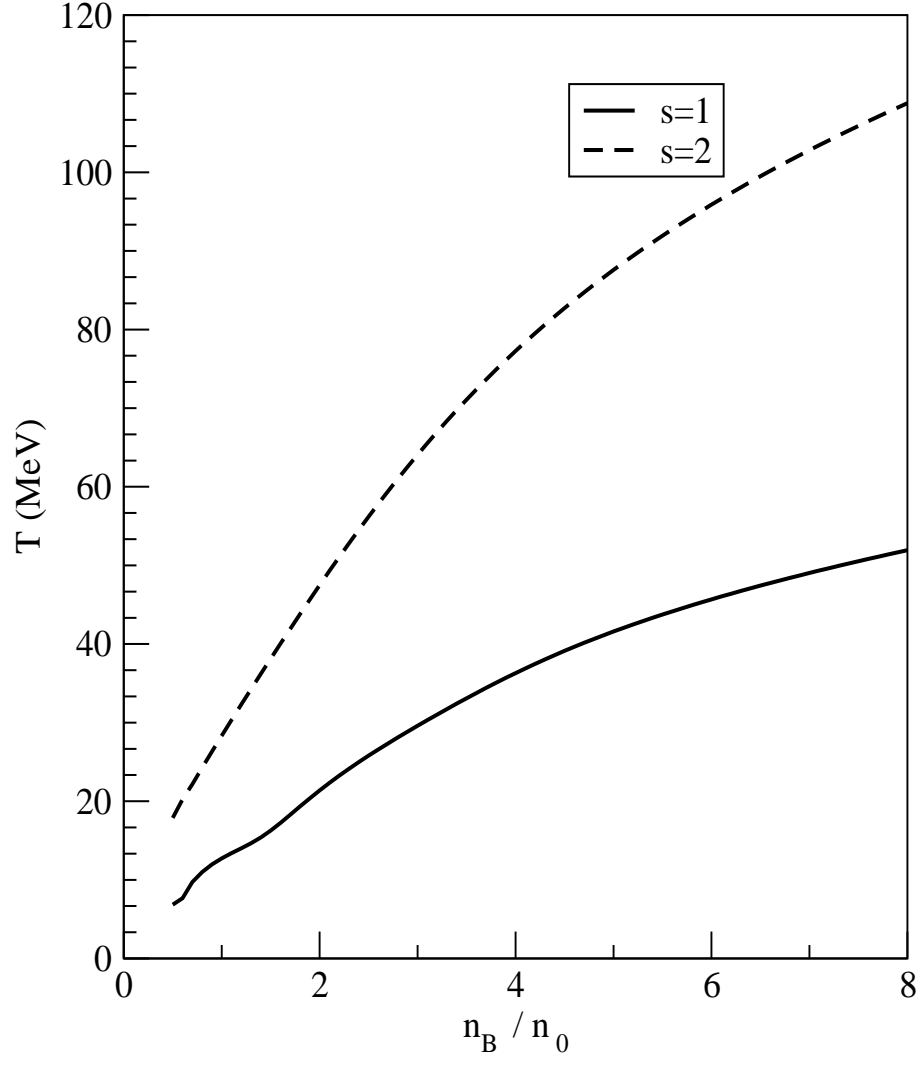


FIG. 1. Temperature is plotted as a function of baryon density for neutrino-free nuclear matter and fixed entropy per baryon  $s = 1$  and 2.

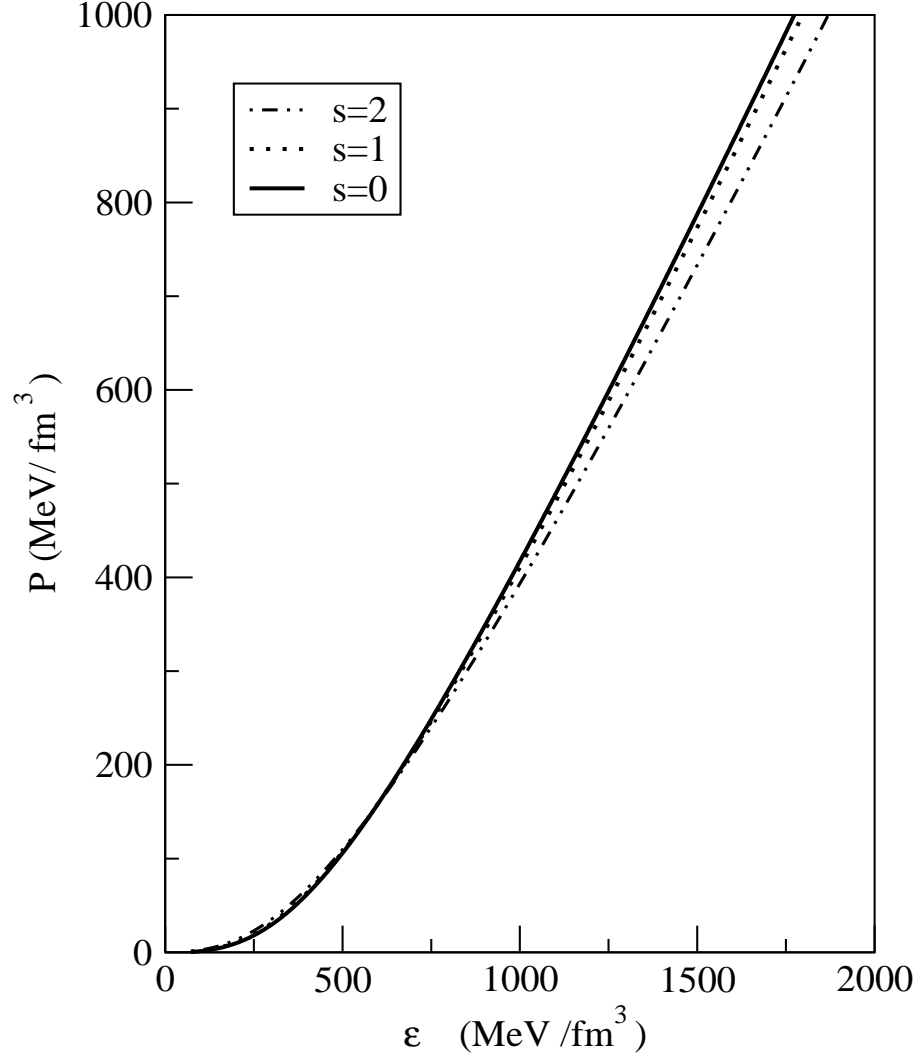


FIG. 2. Pressure is plotted with energy density for neutrino-free nuclear matter and fixed entropy per baryon  $s = 0, 1$ , and  $2$ .

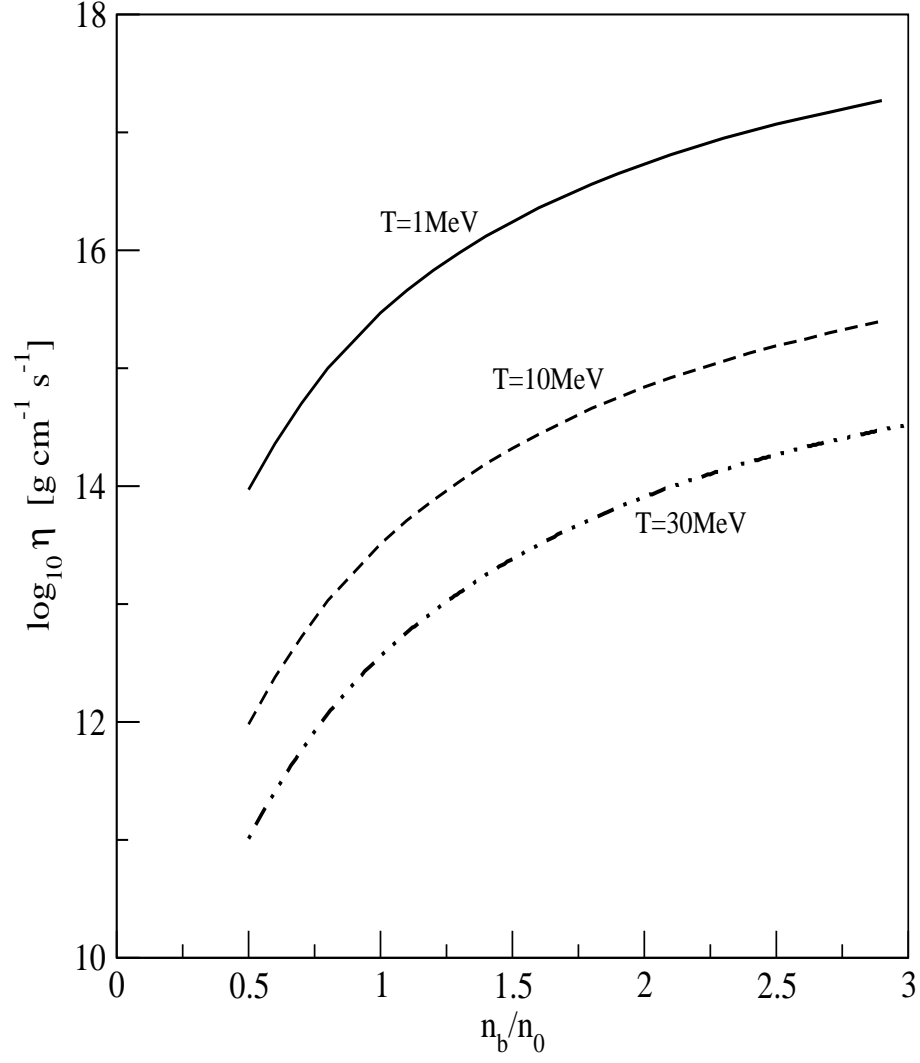


FIG. 3. Total shear viscosity in the nuclear matter phase is plotted with normalised baryon density for different temperatures.



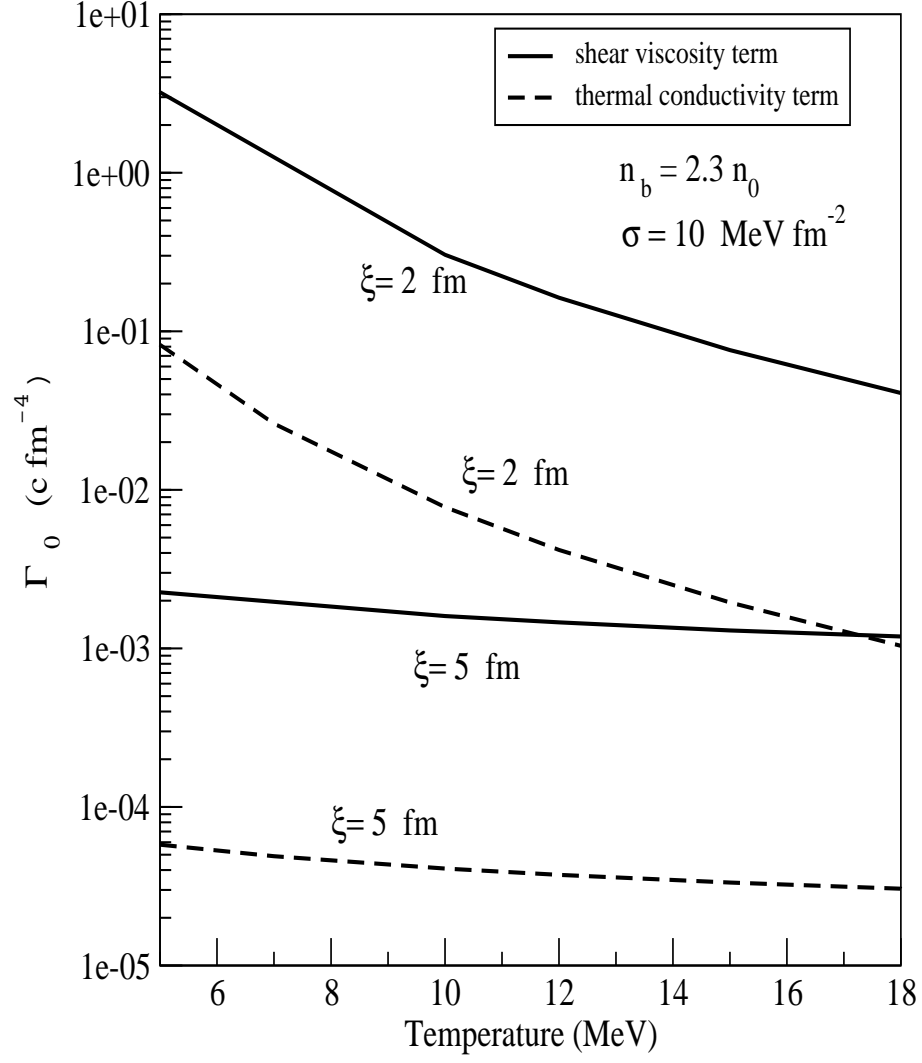


FIG. 4. Prefactor is shown as a function of temperature for different correlation lengths and at a fixed density and surface tension.

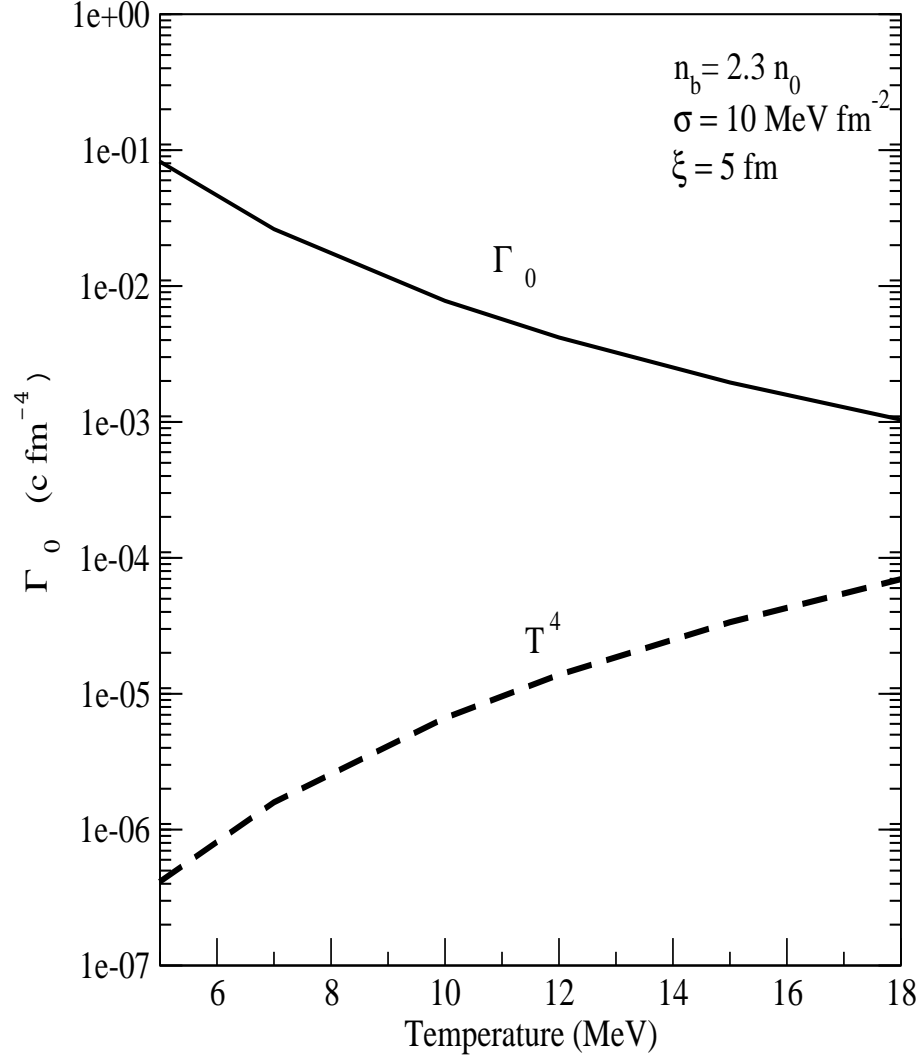


FIG. 5. Same as Fig. 4, but the prefactor including the contribution of shear viscosity is compared with that of  $T^4$  approximation.

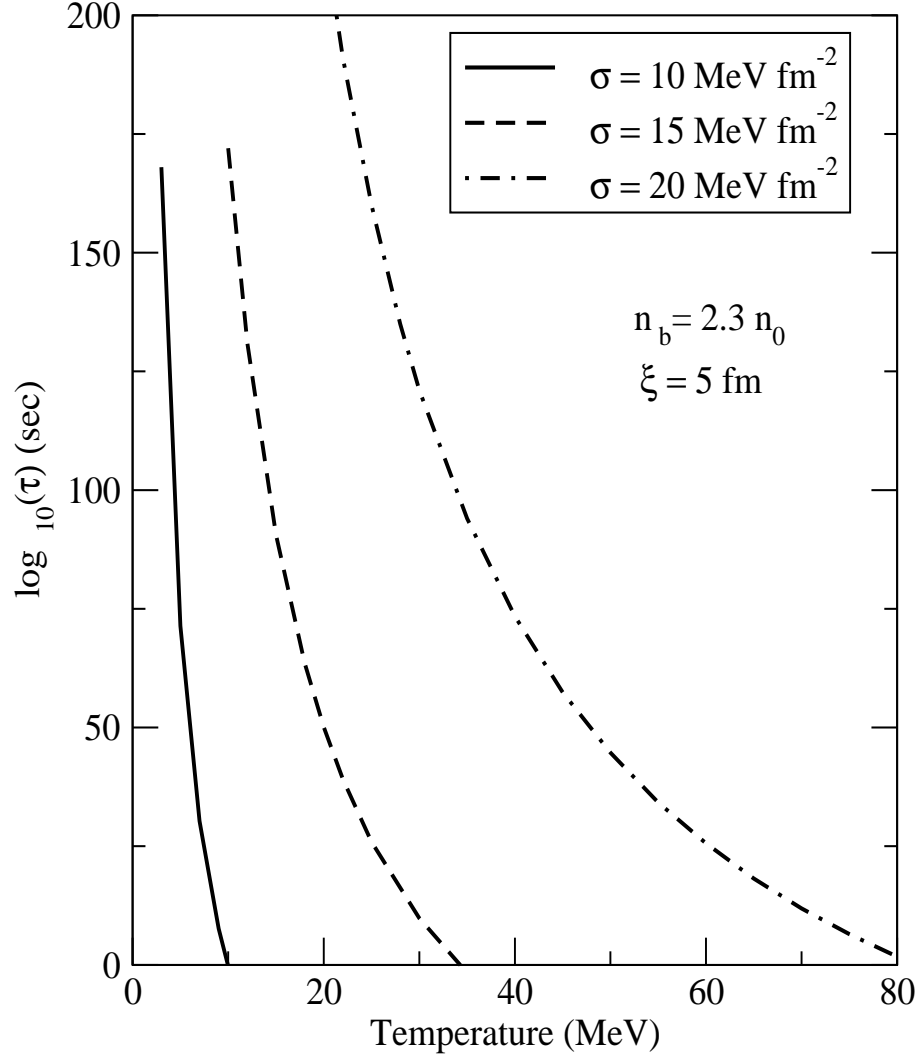


FIG. 6. Thermal nucleation time is displayed with temperature for different values of surface tension.

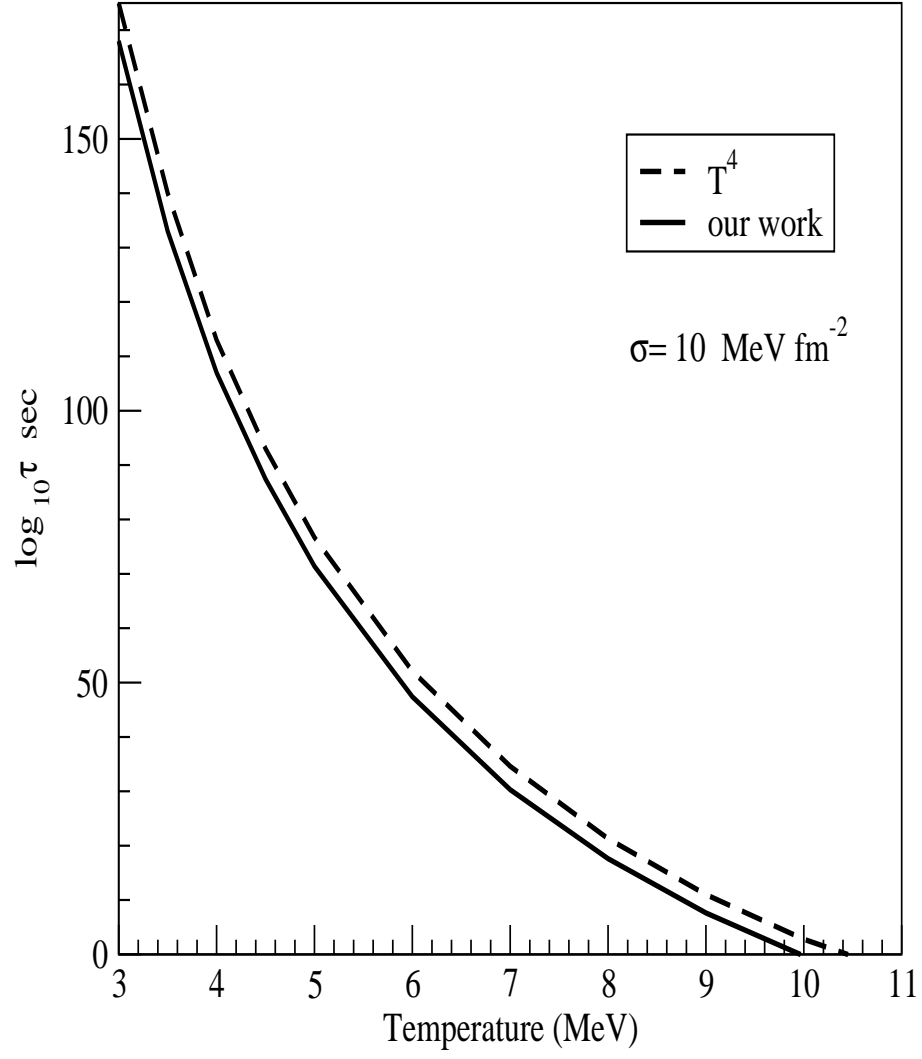


FIG. 7. Same as Fig.6 but our results are compared with the calculation of  $T^4$  approximation.